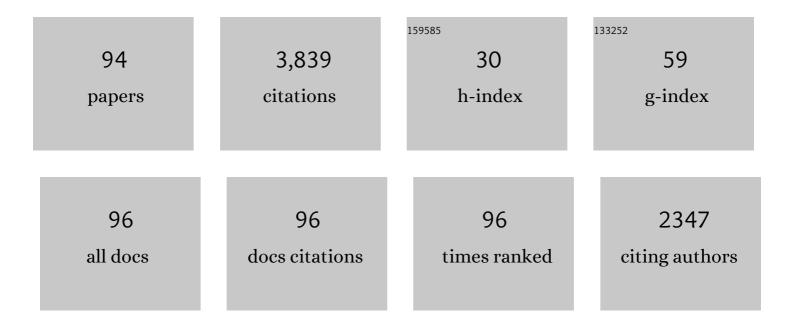
## **Rolf Brendel**

List of Publications by Year in descending order

Source: https://exaly.com/author-pdf/1561562/publications.pdf Version: 2024-02-01



ROLE RDENDEL

#	Article	IF	CITATIONS
1	Laser contact openings for local poly-Si-metal contacts enabling 26.1%-efficient POLO-IBC solar cells. Solar Energy Materials and Solar Cells, 2018, 186, 184-193.	6.2	475
2	Surface passivation of crystalline silicon solar cells: Present and future. Solar Energy Materials and Solar Cells, 2018, 187, 39-54.	6.2	285
3	19%â€efficient and 43 µmâ€ŧhick crystalline Si solar cell from layer transfer using porous silicon. Progress in Photovoltaics: Research and Applications, 2012, 20, 1-5.	8.1	236
4	Recombination behavior and contact resistance of n+ and p+ poly-crystalline Si/mono-crystalline Si junctions. Solar Energy Materials and Solar Cells, 2014, 131, 85-91.	6.2	195
5	Contact Selectivity and Efficiency in Crystalline Silicon Photovoltaics. IEEE Journal of Photovoltaics, 2016, 6, 1413-1420.	2.5	140
6	Ion Implantation for Poly-Si Passivated Back-Junction Back-Contacted Solar Cells. IEEE Journal of Photovoltaics, 2015, 5, 507-514.	2.5	131
7	19.4%â€efficient largeâ€area fully screenâ€printed silicon solar cells. Physica Status Solidi - Rapid Research Letters, 2011, 5, 147-149.	2.4	111
8	A Roadmap Toward 24% Efficient PERC Solar Cells in Industrial Mass Production. IEEE Journal of Photovoltaics, 2017, 7, 1541-1550.	2.5	102
9	Towards 20% efficient largeâ€area screenâ€printed rearâ€passivated silicon solar cells. Progress in Photovoltaics: Research and Applications, 2012, 20, 630-638 A Simple Model Describing the Symmetric &It formula formulatype="inline">&Ittex	8.1	100
10	Notation="TeX">\$Inbox{}V\$ Characteristics of <formula formulatype="inline"&gt;<tex notation="TeX">\$hbox{p}\$</tex> Polycrystalline Si/ <formula formulatype="inline"><tex Notation="TeX"&gt;\$hbox{n}\$</tex </formula> Monocrystalline Si, and <formula< td=""><td>2.5</td><td>91</td></formula<></formula 	2.5	91
11	formulatype="inline"> <tex notation="TeX">\$hbox{n}\$</tex> P. IEEE Jour Junction Resistivity of Carrier-Selective Polysilicon on Oxide Junctions and Its Impact on Solar Cell Performance. IEEE Journal of Photovoltaics, 2017, 7, 11-18.	2.5	91
12	Parasitic Absorption in Polycrystalline Si-layers for Carrier-selective Front Junctions. Energy Procedia, 2016, 92, 199-204.	1.8	77
13	26.1%â€efficient POLOâ€IBC cells: Quantification of electrical and optical loss mechanisms. Progress in Photovoltaics: Research and Applications, 2019, 27, 950-958.	8.1	76
14	Modeling solar cells with the dopantâ€diffused layers treated as conductive boundaries. Progress in Photovoltaics: Research and Applications, 2012, 20, 31-43.	8.1	74
15	Reassessment of intrinsic lifetime limit in n-type crystalline silicon and implication on maximum solar cell efficiency. Solar Energy Materials and Solar Cells, 2018, 186, 194-199.	6.2	66
16	Contact passivation in silicon solar cells using atomicâ€layerâ€deposited aluminum oxide layers. Physica Status Solidi - Rapid Research Letters, 2011, 5, 298-300.	2.4	65
17	Improvement of the SRH bulk lifetime upon formation of n-type POLO junctions for 25% efficient Si solar cells. Solar Energy Materials and Solar Cells, 2017, 173, 85-91.	6.2	65
18	Accurate Calculation of the Absorptance Enhances Efficiency Limit of Crystalline Silicon Solar Cells With Lambertian Light Trapping. IEEE Journal of Photovoltaics, 2018, 8, 1156-1158.	2.5	62

#	Article	IF	CITATIONS
19	21.2%-efficient fineline-printed PERC solar cell with 5 busbar front grid. Physica Status Solidi - Rapid Research Letters, 2014, 8, 675-679.	2.4	61
20	High-rate atomic layer deposition of Al2O3 for the surface passivation of Si solar cells. Energy Procedia, 2011, 8, 301-306.	1.8	60
21	Perimeter Recombination in 25%-Efficient IBC Solar Cells With Passivating POLO Contacts for Both Polarities. IEEE Journal of Photovoltaics, 2018, 8, 23-29.	2.5	49
22	On the recombination behavior of p <sup><i>+</i></sup> -type polysilicon on oxide junctions deposited by different methods on textured and planar surfaces. Physica Status Solidi (A) Applications and Materials Science, 2017, 214, 1700058.	1.8	48
23	Application of a New Ray Tracing Framework to the Analysis of Extended Regions in Si Solar Cell Modules. Energy Procedia, 2013, 38, 86-93.	1.8	45
24	Recombination Behavior of Photolithography-free Back Junction Back Contact Solar Cells with Carrier-selective Polysilicon on Oxide Junctions for Both Polarities. Energy Procedia, 2016, 92, 412-418.	1.8	42
25	Analytical Theory for Extracting Specific Contact Resistances of Thick Samples From the Transmission Line Method. IEEE Electron Device Letters, 2014, 35, 9-11.	3.9	41
26	Breakdown of the efficiency gap to 29% based on experimental input data and modeling. Progress in Photovoltaics: Research and Applications, 2016, 24, 1475-1486.	8.1	41
27	Modeling the Spectral Luminescence Emission of Silicon Solar Cells and Wafers. IEEE Journal of Photovoltaics, 2013, 3, 1038-1052.	2.5	38
28	Evolutionary PERC+ solar cell efficiency projection towards 24% evaluating shadow-mask-deposited poly-Si fingers below the Ag front contact as next improvement step. Solar Energy Materials and Solar Cells, 2020, 212, 110586.	6.2	36
29	High Efficiency N-Type Emitter-Wrap-Through Silicon Solar Cells. IEEE Journal of Photovoltaics, 2011, 1, 49-53.	2.5	34
30	Simulation Tool for Equivalent Circuit Modeling of Photovoltaic Devices. IEEE Journal of Photovoltaics, 2012, 2, 572-579.	2.5	32
31	Direct Laser Texturing for High-Efficiency Silicon Solar Cells. IEEE Journal of Photovoltaics, 2013, 3, 656-661.	2.5	31
32	Backâ€contacted bottom cells with three terminals: Maximizing power extraction from currentâ€mismatched tandem cells. Progress in Photovoltaics: Research and Applications, 2019, 27, 410-423.	8.1	31
33	UV-induced degradation of PERC solar modules with UV-transparent encapsulation materials. Progress in Photovoltaics: Research and Applications, 2017, 25, 409-416.	8.1	29
34	From PERC to Tandem: POLO- and p <sup>+</sup> /n <sup>+</sup> Poly-Si Tunneling Junction as Interface Between Bottom and Top Cell. IEEE Journal of Photovoltaics, 2019, 9, 49-54.	2.5	29
35	For none, one, or two polarities—How do POLO junctions fit best into industrial Si solar cells?. Progress in Photovoltaics: Research and Applications, 2020, 28, 503-516.	8.1	28
36	Emitter saturation current densities of 22 fA/cm <sup>2</sup> applied to industrial PERC solar cells approaching 22% conversion efficiency. Progress in Photovoltaics: Research and Applications, 2017, 25, 509-514.	8.1	26

#	Article	IF	CITATIONS
37	Thin macroporous silicon heterojunction solar cells. Physica Status Solidi - Rapid Research Letters, 2012, 6, 187-189.	2.4	24
38	Simulation-based roadmap for the integration of poly-silicon on oxide contacts into screen-printed crystalline silicon solar cells. Scientific Reports, 2021, 11, 996.	3.3	24
39	High-Efficiency Cells From Layer Transfer: A First Step Toward Thin-Film/Wafer Hybrid Silicon Technologies. IEEE Journal of Photovoltaics, 2011, 1, 9-15.	2.5	23
40	Optimized Interconnection of Passivated Emitter and Rear Cells by Experimentally Verified Modeling. IEEE Journal of Photovoltaics, 2016, 6, 432-439.	2.5	23
41	Firing-Stable PECVD SiO <i><sub>x</sub></i> N <i><sub>y</sub></i> /n-Poly-Si Surface Passivation for Silicon Solar Cells. ACS Applied Energy Materials, 2021, 4, 4646-4653.	5.1	22
42	Ultraâ€Thin Polyâ€&i Layers: Passivation Quality, Utilization of Charge Carriers Generated in the Polyâ€&i and Application on Screenâ€Printed Doubleâ€&ide Contacted Polycrystalline Si on Oxide Cells. Solar Rrl, 2020, 4, 2000177.	5.8	21
43	Aluminum-Based Mechanical and Electrical Laser Interconnection Process for Module Integration of Silicon Solar Cells. IEEE Journal of Photovoltaics, 2012, 2, 16-21.	2.5	20
44	Modeling recombination and contact resistance of poly‣i junctions. Progress in Photovoltaics: Research and Applications, 2020, 28, 1289-1307.	8.1	20
45	Modeling the formation of local highly aluminum-doped silicon regions by rapid thermal annealing of screen-printed aluminum. Physica Status Solidi - Rapid Research Letters, 2012, 6, 111-113.	2.4	19
46	Building Blocks for Industrial, Screen-Printed Double-Side Contacted POLO Cells With Highly Transparent ZnO:Al Layers. IEEE Journal of Photovoltaics, 2018, , 1-7.	2.5	19
47	High Temperature Annealing of ZnO:Al on Passivating POLO Junctions: Impact on Transparency, Conductivity, Junction Passivation, and Interface Stability. IEEE Journal of Photovoltaics, 2019, 9, 89-96.	2.5	19
48	Changes in hydrogen concentration and defect state density at the poly-Si/SiOx/c-Si interface due to firing. Solar Energy Materials and Solar Cells, 2021, 231, 111297.	6.2	19
49	Detailed Analysis and Understanding of the Transport Mechanism of Poly-Si-Based Carrier Selective Junctions. IEEE Journal of Photovoltaics, 2019, 9, 1575-1582.	2.5	18
50	Degradation and Regeneration of <i>n</i> <sup>+</sup> -Doped Poly-Si Surface Passivation on <i>p</i> -Type and <i>n</i> -Type Cz-Si Under Illumination and Dark Annealing. IEEE Journal of Photovoltaics, 2020, 10, 423-430.	2.5	17
51	Macroporous Silicon Solar Cells With an Epitaxial Emitter. IEEE Journal of Photovoltaics, 2013, 3, 723-729.	2.5	16
52	Numerical simulations of buried emitter backâ€junction solar cells. Progress in Photovoltaics: Research and Applications, 2009, 17, 253-263.	8.1	15
53	21.0%-efficient screen-printed n-PERT back-junction silicon solar cell with plasma-deposited boron diffusion source. Solar Energy Materials and Solar Cells, 2016, 158, 50-54.	6.2	15
54	Emitter recombination current densities of boron emitters with silver/aluminum pastes. , 2014, , .		13

#	Article	IF	CITATIONS
55	A 22.3% Efficient pâ€Type Back Junction Solar Cell with an Alâ€Printed Frontâ€Side Grid and a Passivating n <sup>+</sup> â€Type Polysilicon on Oxide Contact at the Rear Side. Solar Rrl, 2020, 4, 2000435.	5.8	13
56	The origin of reduced fill factors of emitter-wrap-through-solar cells. Physica Status Solidi - Rapid Research Letters, 2008, 2, 251-253.	2.4	12
57	Al-Foil on Encapsulant for the Interconnection of Al-Metalized Silicon Solar Cells. IEEE Journal of Photovoltaics, 2013, 3, 77-82.	2.5	12
58	Lambertian light trapping in thin crystalline macroporous Si layers. Physica Status Solidi - Rapid Research Letters, 2014, 8, 235-238.	2.4	12
59	Industrial bifacial n-type silicon solar cells applying a boron co-diffused rear emitter and an aluminum rear finger grid. Physica Status Solidi (A) Applications and Materials Science, 2016, 213, 3046-3052.	1.8	12
60	Firing stability of tube furnaceâ€annealed nâ€ŧype polyâ€Si on oxide junctions. Progress in Photovoltaics: Research and Applications, 2022, 30, 49-64.	8.1	12
61	UV radiation hardness of photovoltaic modules featuring crystalline Si solar cells with AlO <i><sub>x</sub></i> /p <sup>+</sup> â€ŧype Si and SiN <i><sub>y</sub></i> /n <sup>+</sup> â€ŧype Si interfaces. Physica Status Solidi - Rapid Research Letters, 2017, 11, 1700178.	2.4	11
62	Rear-side point-contacts by inline thermal evaporation of aluminum. , 2010, , .		10
63	19% Efficient Thin-Film Crystalline Silicon Solar Cells From Layer Transfer Using Porous Silicon: A Loss Analysis by Means of Three-Dimensional Simulations. IEEE Transactions on Electron Devices, 2012, 59, 909-917.	3.0	10
64	Interconnection of busbarâ€free back contacted solar cells by laser welding. Progress in Photovoltaics: Research and Applications, 2015, 23, 1057-1065.	8.1	10
65	Fully screenâ€printed silicon solar cells with local Alâ€p <sup>+</sup> and nâ€type POLO interdigitated back contacts with a <i>V</i> <sub>OC</sub> of 716 mV and an efficiency of 23%. Progress in Photovoltaics: Research and Applications, 2021, 29, 516-523.	8.1	10
66	Modelling c‣i/SiN <i><sub>x</sub></i> interface recombination by surface damage. Physica Status Solidi - Rapid Research Letters, 2010, 4, 91-93.	2.4	9
67	Ion implantation of boric molecules for silicon solar cells. Solar Energy Materials and Solar Cells, 2015, 142, 12-17.	6.2	9
68	Directional Heating and Cooling for Controlled Spalling. IEEE Journal of Photovoltaics, 2015, 5, 195-201.	2.5	9
69	On the chances and challenges of combining electronâ€collecting <i>n</i> POLO and holeâ€collecting Alâ€ <i>p</i> <sup>+</sup> contacts in highly efficient <i>p</i> â€type câ€6i solar cells. Progress in Photovoltaics: Research and Applications, 2023, 31, 327-340.	8.1	9
70	21.0%-efficient co-diffused screen printed n-type silicon solar cell with rear-side boron emitter. Physica Status Solidi - Rapid Research Letters, 2016, 10, 148-152.	2.4	8
71	Reuse of Substrate Wafers for the Porous Silicon Layer Transfer. IEEE Journal of Photovoltaics, 2016, 6, 783-790.	2.5	8
72	Impact of Contacting Geometries When Measuring Fill Factors of Solar Cell Current–Voltage Characteristics. IEEE Journal of Photovoltaics, 2017, 7, 747-754.	2.5	8

#	Article	IF	CITATIONS
73	Laser transfer doping for contacting n-type crystalline Si solar cells. Physica Status Solidi (A) Applications and Materials Science, 2011, 208, 1964-1966.	1.8	7
74	Al <sup>+</sup> -doping of Si by laser ablation of Al <sub>2</sub> O <sub>3</sub> /SiN passivation. Physica Status Solidi (A) Applications and Materials Science, 2013, 210, 1871-1873.	1.8	7
75	Bow of Silicon Wafers After In-Line High-Rate Evaporation of Aluminum. IEEE Journal of Photovoltaics, 2013, 3, 212-216.	2.5	6
76	A Cross-Country Model for End-Use Specific Aggregated Household Load Profiles. Energies, 2021, 14, 2167.	3.1	6
77	Optimizing the geometry of local aluminum-alloyed contacts to fully screen-printed silicon solar cells. , 2012, , .		5
78	Aluminum Evaporation and Etching for the Front-Side Metallization of Solar Cells. IEEE Journal of Photovoltaics, 2013, 3, 702-708.	2.5	5
79	Contacting a single nanometerâ€sized pinhole in the interfacial oxide of a polyâ€silicon on oxide (POLO) solar cell junction. Progress in Photovoltaics: Research and Applications, 2021, 29, 936-942.	8.1	5
80	Light and elevated temperature induced degradation and recovery of gallium-doped Czochralski-silicon solar cells. Scientific Reports, 2022, 12, 8089.	3.3	5
81	Light Trapping and Surface Passivation of Micron-Scaled Macroporous Blind Holes. IEEE Journal of Photovoltaics, 2016, 6, 397-403.	2.5	4
82	Simulation of optical properties of Si wire cells. , 2009, , .		3
83	Large area macroporous silicon layers for monocrystalline thin-film solar cells. , 2010, , .		3
84	Influence of emitter profile characteristics on thermal stability and passiviation quality of a-Si/SiN <inf>X</inf> -passivated boron emitters. , 2010, , .		3
85	From highâ€efficiency <i>n</i> â€type solar cells to modules exceeding 20% efficiency with aluminumâ€based cell interconnection. Progress in Photovoltaics: Research and Applications, 2013, 21, 1354-1362.	8.1	3
86	Analysis of Thermal Processes Driving Laser Welding of Aluminum Deposited on Glass Substrates for Module Interconnection of Silicon Solar Cells. IEEE Journal of Photovoltaics, 2015, 5, 1606-1612.	2.5	3
87	Evaluation of localized vertical current formation in carrier selective passivation layers of silicon solar cells by conductive AFM. AIP Conference Proceedings, 2019, , .	0.4	3
88	Impact of Local Back-Surface-Field Thickness Variation on Performance of PERC Solar Cells. IEEE Journal of Photovoltaics, 2021, 11, 908-913.	2.5	3
89	Contact resistance of local rear side contacts of screen-printed silicon PERC solar cells with efficiencies up to 19.4%. , 2011, , .		2
90	High efficiency n-type emitter-wrap-through silicon solar cells. , 2011, , .		2

High efficiency n-type emitter-wrap-through silicon solar cells. , 2011, , . 90

#	Article	IF	CITATIONS
91	Macroporous silicon as an absorber for thin heterojunction solar cells. , 2012, , .		2
92	Laser microwelding of thin Al layers for interconnection of crystalline Si solar cells: analysis of process limits for ns and μs lasers. Journal of Photonics for Energy, 2014, 4, 041597.	1.3	1
93	Thermal processes driving laser-welding for module interconnection. , 2015, , .		1
94	Epitaxial Si films carried by thick polycrystalline Si as a drop-in replacement for conventional Si wafers. , 2014, , .		0